



A REALISTIC FULL CFRP RETROFIT OF RC BEAM-COLUMN JOINTS COMPARED TO SEISMICALLY DESIGNED SPECIMENS

D.A. Pohoryles⁽¹⁾, J. Melo⁽²⁾, T. Rossetto⁽³⁾, H. Varum⁽⁴⁾, D. D'Ayala⁽³⁾

⁽¹⁾ Ph.D. Candidate, EPICentre, University College London, U.K., daniel.pohoryles.10@ucl.ac.uk

⁽²⁾ Research Associate, EPICentre, University College London, U.K., jose.melo.11@ucl.ac.uk

⁽³⁾ Professor, EPICentre, University College London, U.K.

⁽⁴⁾ Professor, CONSTRUCT, Faculty of Engineering of the University of Porto, Portugal

Abstract

The brittle collapse of reinforced concrete (RC) structures built before the introduction of detailed seismic design codes (pre-1970's) in recent earthquakes, has underlined the need for significant upgrades to the existing RC building stock. In particular, the observation of weak-column/strong-beam mechanisms has potentially catastrophic impacts that could be addressed by retrofit solutions. Retrofits with fibre reinforced polymers (FRP) have become increasingly popular and experimental evidence for their effectiveness can be found in the literature. The lack of tests on full-scale specimens with slabs and transverse beams in many studies may however lead to an unrealistic assessment of FRP retrofit schemes. In this study, three realistic full-scale interior beam-column joints with slab and transverse beams are tested under cyclic loading in order to propose and assess practical FRP retrofit solutions. A complete Carbon FRP (CFRP) retrofit strategy aiming to obtain a similar performance to a specimen designed to modern European design guidelines (Eurocode 8) is presented. The retrofit scheme is composed of selective strengthening and weakening components to ensure ductile failure of the specimen according to capacity design principles. Results from full-scale cyclic tests on the CFRP retrofitted specimen are compared to the behaviour of a deficient, pre-1970's design specimen and a specimen designed to modern guidelines. The observed failure mechanisms and global lateral capacities for the Eurocode 8 and retrofitted specimen show that the CFRP retrofit is effective in improving seismic behaviour. By means of a combined selective weakening and strengthening scheme, a change in hierarchy of strengths can be achieved, which leads to an improved ductile behaviour with significant strength enhancement. The results suggest that a CFRP retrofit scheme can be devised for realistic, significantly under-designed structures in order to achieve a similar performance to modern RC structures designed to sophisticated seismic guidelines.

Keywords: FRP; Seismic retrofit; Beam-column joint; Full-scale testing; Existing structures; RC structures



1. Introduction

Observations of severe damage to existing reinforced concrete (RC) structures in recent earthquake events have highlighted significant structural deficiencies in buildings designed before the 1970's. As a result of non-compliance with the capacity design approach, brittle failures such as weak-column/strong-beam mechanisms are often observed [1]. For a large proportion of the existing RC building stock in seismic regions, ductility and lateral strength are limited due to their deficient design. Retrofit solutions are hence required to reduce significant human and economic losses in future events.

Since the significant repair and retrofit efforts following the 2009 L'Aquila, Italy, and 2011 Christchurch, NZ, earthquakes, fibre reinforced polymers (FRP) are considered as viable alternative strengthening materials to traditional concrete or steel jacketing. In the field, FRP retrofits at component-level (beam or column) are commonly implemented. Moreover, experimental efforts to modify the hierarchy of strength according to capacity design principles, by enhancing the shear capacity of unreinforced joints or by confining and strengthening columns can be found in the literature [2]. Close to 200 published tests on non-seismically designed RC joints retrofitted with FRP have been compiled in a database by the authors. A statistical analysis of this database highlights that a majority of tests in the literature do not reflect real conditions, as the specimens have scaled dimensions (60% of all tested specimens) or do not include slabs or transverse beams in the set-up (85%). The presence of slabs and transverse beams in real structures however lead to practical challenges to the application of retrofit solutions, including the wrapping of members, continuity of flexural strengthening and anchorage. Moreover, these factors significantly influence the failure mechanism of joints, hence affecting the design and effectiveness of FRP retrofits [3–5].

Two experimental studies on pre-1970's full-scale interior beam-column joints with slab and transverse beams were initially conducted to test the effectiveness of FRP retrofits in a set-up reflecting real structures [6,7]. The first study demonstrated that an FRP retrofit with continuous column strengthening through the slab and confinement of the column plastic hinge zones can prevent brittle single-storey failures and column bar buckling [6]. This retrofit does however not achieve a reversal of the hierarchy of strengths between column and beams due to the strong contribution of the slab hindering rotation of the beams.

A second retrofit for realistic interior joints aimed to increase ductility and alter the failure mechanism [7]. In this case a combination of a CFRP column retrofit with selective weakening (SW) was implemented to reduce the floor slab contribution by cutting the slab reinforcement along the potential plastic hinge zone of the beam. This was previously shown effective for corner beam-column joints [8]. This retrofit successfully reversed the hierarchy of strength with the behaviour of the strengthened specimen characterised by a ductile, beam-dominated failure mechanism. This retrofit does however not result in any significant increase in strength of the specimen and joint damage was observed.

In this paper, results from full-scale cyclic testing of a new retrofit scheme for realistic RC beam-column joints are presented. Based on the outcomes of the two former studies, a realistic CFRP strengthening of columns, beams and joint combined with selective weakening of the slab is postulated. The proposed intervention aims to significantly increase the lateral capacity of the specimen, while ensuring a change in failure mechanism to a ductile weak-beam/strong-column failure mechanism. The results of the retrofitted specimen are compared to the behaviour of a deficient, pre-1970's design specimen and a specimen designed to modern seismic guidelines (Eurocode 8).

2. Methodology

2.1 Test specimens and materials

The three specimens presented in this study are two control specimens, C1 and C-EC8, and one retrofit specimen, C1-RT-B-sw. The label 'sw' refers to selective weakening of the slab. The specimens are designed to represent real-scale interior beam-column joints in a four-storey RC frame structure, as shown in Fig. 1. The superior and inferior columns represent a half-storey 1.50 m column with a square cross-section of 300 mm by 300 mm.

Similarly, each beam represents a 2.00 m rectangular half-span beam with a cross-section of 450 mm deep to 300 mm wide. The slab has a depth of 150 mm and is 1.95 m wide.

The monitoring set-up for the experiments aims to provide more in-depth information on the behaviour of the specimens. It includes eight strain gauges on the reinforcement (on the superior column, inferior column, and beam top and bottom bars), four strain gauges on the vertical FRP, 16 LVDT's, 28 rectilinear displacement transducers, four draw-wire position transducers and four inductive linear position sensors, as well as six cameras for strain measurements using digital image correlation.

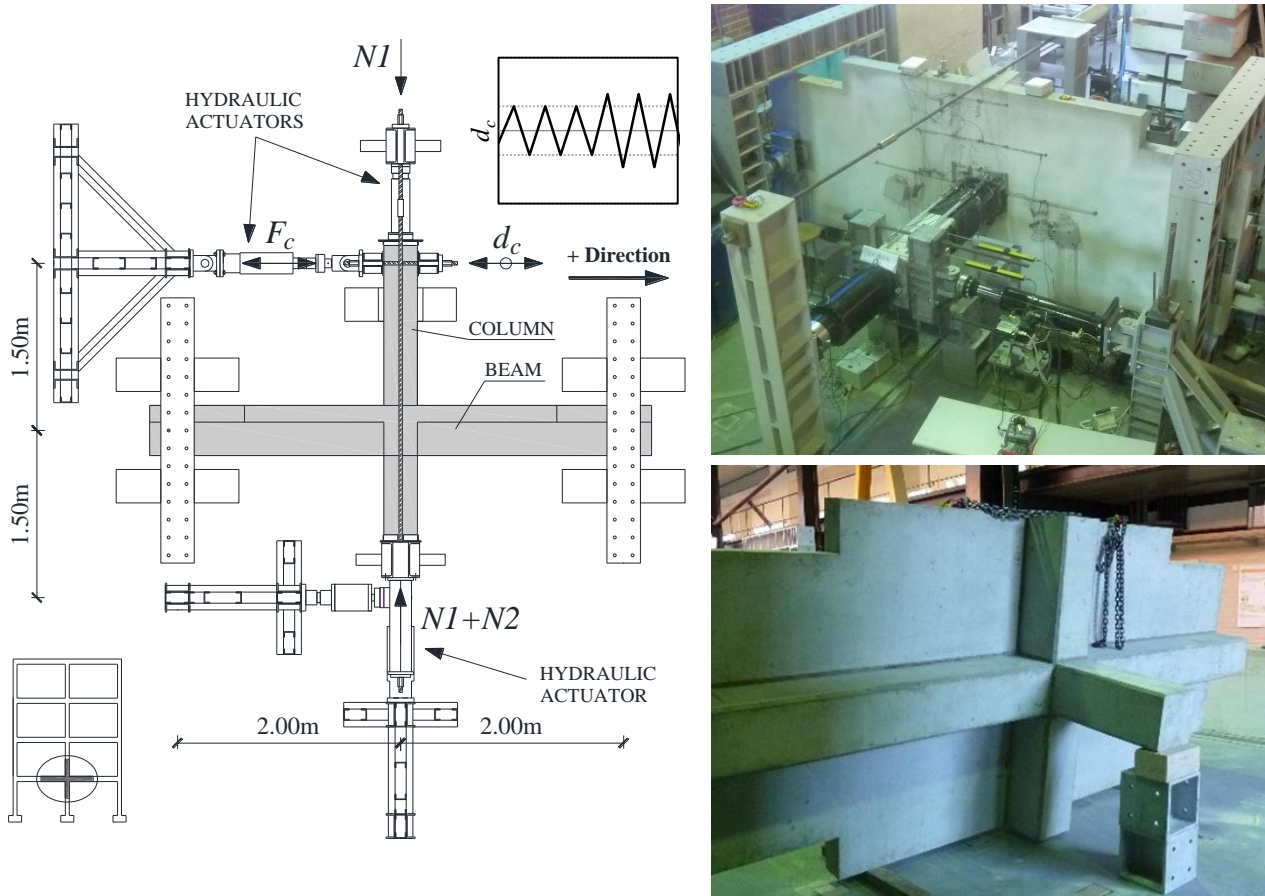


Fig. 1. Test-set up, prototype structure and sample of loading protocol.

The reinforcement detailing adopted in the specimens can be seen in Fig. 2. The design for C1 and C1-RT-B-sw are shown on the right side of the figure and reflect common design practice for a pre-1970's RC building in a Mediterranean country. As a representative example, the design follows the REBA Portuguese code (1967), which adopts a seismic coefficient for lateral load of 0.05 of the axial load. Typical design deficiencies compared to modern design practice include an inappropriate hierarchy of strengths (weak- column/strong-beam) and a lack of reinforcement of the joint, as well as a limited confinement in the columns due to inadequate transverse reinforcement spacing. Specimen C-EC8, in turn, is designed to modern seismic design provisions in a highly seismic zone and follows Eurocode 8 [9].

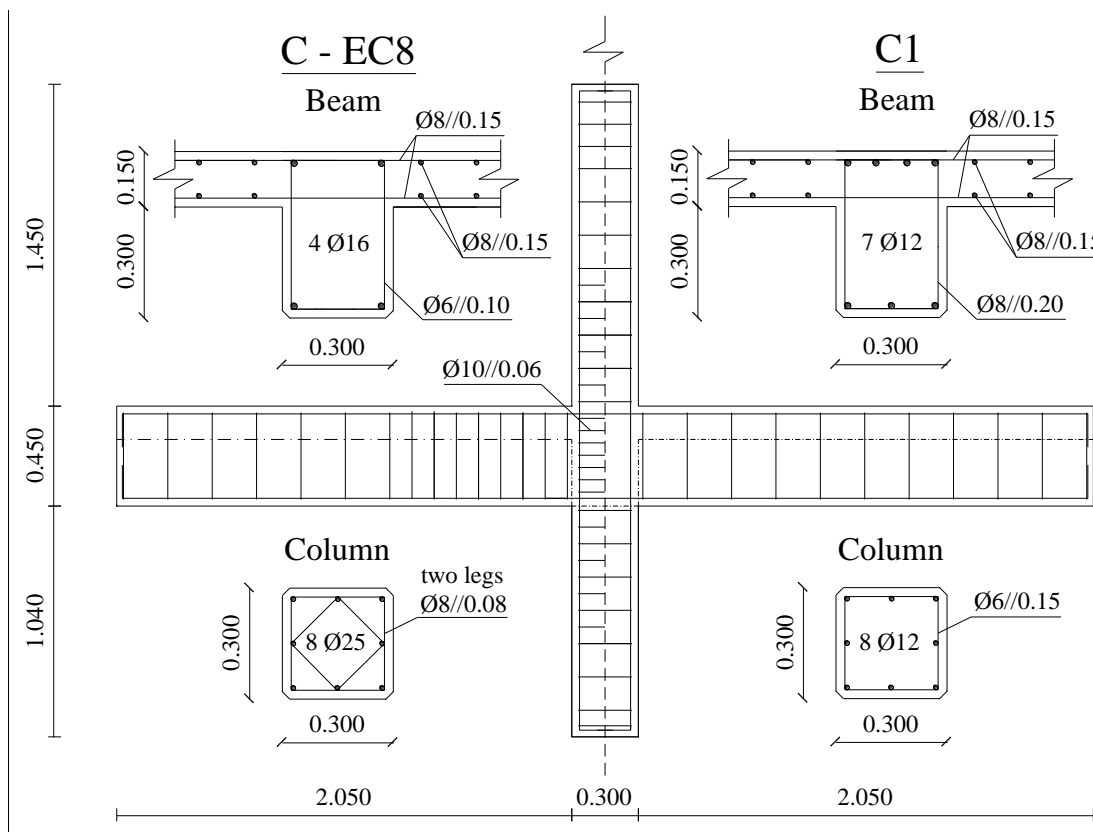


Fig. 2. Reinforcement detailing for specimens C-EC8 (left) and C1 and C1-RT-B (right) - dimensions in m

The mean values of the material properties for the three test specimens are summarised in Table 1. Results from compressive cylinder tests ($\varnothing 150 \times 300 \text{ mm}^2$), as well as tensile strength tests on steel and CFRP are reported. The CFRP sheets used for retrofit are S&P C-240 sheets with a thickness of 0.223 mm per layer. For the CFRP tensile strength, the method in ISO/DIS 10406-2:2013 is adopted.

Table 1. Material properties for beam-column joint specimens.

| Specimen | f_{cm} (MPa) | Steel f_y/f_u (MPa) | | | | | | $f_{u,FRP}$ (MPa) | $\varepsilon_{u,FRP}$ (%) |
|------------|-------------------|-----------------------|---------|---------|---------|---------|---------|----------------------|------------------------------|
| | | Φ25 | Φ16 | Φ12 | Φ10 | Φ8 | Φ6 | | |
| C1 | 23.4 | | | 450/570 | | 540/640 | 538/645 | | |
| C1-RT-B-sw | 19.3 | | | 450/570 | | 540/640 | 538/645 | 3300 | 1.7 |
| C-EC8 | 32.7 | 530/620 | 530/620 | | 530/620 | 540/640 | 538/645 | | |

2.2 FRP retrofit scheme

In this study, a retrofit scheme (RT-B-sw) compliant with current design recommendations [10,11] is proposed. The design of the retrofit scheme is based on observations from the literature [12,13] and previous testing [6,7], as well as recommendations in the latest draft of the ACI guidelines [14]. The main observations influencing this design are summarised below:

1. Continuity of the longitudinal strengthening is required through the beam-column joint and this can be achieved by means of FRP “strands” (see Fig. 3).
2. For realistic specimens with slabs, a change in failure mechanism to comply with capacity design objectives can only be achieved by “selective weakening” of the slab, i.e. cutting through the slab reinforcement close to the joint. This does not affect the serviceability performance of the slab as the cuts are not in a zone of high moments under gravity loading.
3. Strengthening and confinement of the beams close to the joint is required for plastic hinge relocation within the beam and protection from plasticity spreading into the joint.
4. Joint strengthening is required when increasing the overall lateral capacity of the specimens.



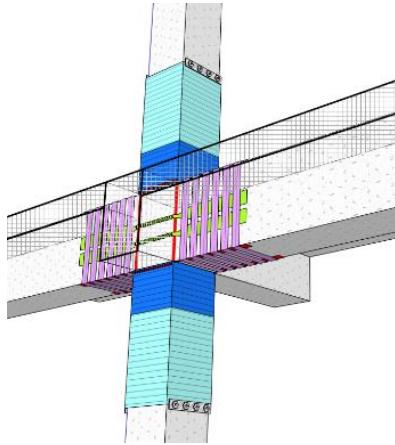
Fig. 3. FRP “strand”: rolled FRP sheet passed through plastic tube

The objective of retrofit scheme B-sw is to achieve a similar performance to a structure designed to modern guidelines (C-EC8). In particular, the retrofit aims to increase the strength of the sub-assembly to reach a level close to 80% of C-EC8, while achieving ductile failure by promoting the formation of a beam-sway mechanism with a plastic hinge forming in the beams, at one beam-depth (450 mm) from the beam-joint interface. To achieve this, the step-wise retrofit presented in Fig. 4 is proposed.

Following the design philosophy in Eurocode 8, FRP flexural strengthening of columns, as well as confinement and shear strengthening are applied to attain a strong-column/weak-beam mechanism. To achieve continuous flexural strengthening through the slab and joint, vertical FRP strands are used to connect the bottom and top column retrofit. In order to move the plastic hinge to the beam, away from the joint interface, next to FRP strengthening, selective weakening of the slab is performed by means of cutting the slab reinforcement in the potential plastic hinge zone.

The relative strength of the retrofitted members is evaluated by non-linear FE modelling and current guideline equations [11] in order to ensure the capacity of the retrofitted columns is higher than that of the beams by a factor greater than 1.3. From this evaluation, a total of six layers of vertical FRP over a length of 750 mm and three layers of horizontal strengthening are required for the columns, while two 100 mm wide strips are applied in the beams over a length of 450 mm. The transverse strengthening of the beams consists of 50 mm wide strips spaced at 75 mm and is applied as full wraps through holes in the slabs. Finally, as the specimen is designed to pre-seismic design codes, the joint shear capacity is very low and FRP strengthening of the joint by means of horizontal strands through its core is also provided. This consists of two 150 mm wide strips that are extended for 300 mm onto the beams for anchorage. All FRP sheets are additionally anchored using bolted steel plates to avoid end-debonding.

Schematic of retrofit RT-B-sw



Step 1: Selective weakening cuts and holes for FRP strands



Step 2: Application of a base layer of FRP on the column



Steps 3 & 4: Application of FRP strands through slab, splayed out onto columns



Step 5: Column confinement and shear strengthening



Step 6: Strengthening of beams and joint with FRP strands



Step 7: Application of strips of FRP for shear strengthening and anchorage in beams; additional anchorage with bolted steel plates



Fig. 4. Step-wise retrofit of specimen C1-RT-B-sw

3. Results

In this section, results from three full-scale tests are presented. The global lateral force–displacement behaviour is compared, as well as a number of criteria summarised in Table 2. The yield drift, Δ_y , is when the first strain gauge reading exceeds the steel yield strain (0.2%), while the ultimate drift, Δ_u , occurs at a strength reduction of 20% (F_u) from the maximum force (F_{max}) [15]. The ultimate displacement ductility, $\mu_{\Delta u}$, is defined as the ratio between Δ_u and Δ_y . The post-peak softening slope (PPS) is defined as the slope between F_{max} and F_u , and is an indirect measure of residual strength of a structure. The global energy dissipation is defined as the integral of the force-displacement curve, while the energy dissipated by individual members (columns and beams), presented in Fig. 9, is calculated from the moment-rotation curves along the length of the members. Finally, the specimen's behaviour upon repeated cyclic loading is evaluated in terms of inter-cycle strength degradation (ICSD), i.e. the reduction in strength at the end of the 1st and 2nd cycles at each level of drift.

Table 2. Summary of main experimental results (difference to C1 in brackets).

| Specimen | F_{max} (kN) | Failure location | Δ_y (%) | $\mu_{\Delta u}$ | Dissipated Energy (kN.m) | PPS (kN/mm) | ICSD max. (%) |
|------------|-------------------|------------------------|-------------------|------------------|-----------------------------|-------------------|---------------------|
| C1 | 63.1 | Superior Column | 0.65 | 3.6 | 32.1 | -0.49 | -23.22 |
| C-EC8 | 123.9 (+96.4%) | Both Columns, Beams | 0.85 (+30%) | 6.1 (+69.1%) | 172.3 (+437.1%) | -0.47 (-5.8%) | -10.57 (-54.5%) |
| C1-RT-B-sw | 86.9 (+37.7%) | Beams | 0.95 (+46%) | 6.9 (+89.6%) | 111.6 (+247.8%) | -0.19 (-61.8%) | -8.87 (-61.8%) |

3.1 Control specimens

The results for two control specimens are presented in this section. For C1, the specimen designed to pre-1970's guidelines, a brittle failure mechanism dominated by plastic hinge formation and buckling of the superior column bars is observed. As shown in Fig. 5, very limited damage is observed in the rest of the specimen. In a full structure this type of mechanism would lead to a single-storey failure. Due to the contribution of the slab, limited rotation of the beams and no yielding of beam bars are observed. After plastic hinge formation in the column, the ultimate state is reached by concrete crushing and buckling of the column bars just above the column-slab interface. As expected for a non-seismically designed structure, a relatively low lateral capacity of 63.1 kN, as well as a very low ultimate drift (2.3%) and displacement ductility (3.6) are recorded for C1. As shown in Table 2, the inadequate seismic performance of the specimen is underlined by a very low energy dissipation (32.1 kN.m) and large post-peak softening, indicating a low residual strength.



Fig. 5. Final damage state in C1; left: superior column, right: beam underside

For the control specimen designed to Eurocode 8, C-EC8, as expected, a much better cyclic performance is observed. It presents much higher strength of 123.9 kN (+96.4% compared to C1) and a larger ductility of 6.1 (+69.1%). This improvement is associated to a more ductile failure mechanism, with damage spread over a larger area in both beams and columns (Fig. 6). Yielding of reinforcement bars is initially recorded in the bottom beam (0.85%), with yielding of column bars occurring at higher levels of drift (1.6%). The improved failure mechanism is also characterized by a much improved dissipated energy (+437.1%), reduced post-peak softening (-5.8%) and inter-cycle strength degradation (-54.5%). Overall, an improved seismic performance is hence observed.

The final damage state, shown in Fig. 6, reveals that despite adhering to capacity design principles, the ultimate failure is governed by the columns, with visible concrete crushing at the column-joint interfaces. This can be attributed to a stronger slab contribution, as well as a higher over-strength of the beam bars than anticipated by the Eurocode 8 design equations (see [16]). Still, damage in the columns is symmetric in the inferior and superior columns and no buckling is observed, corresponding to a significant improvement compared to C1.

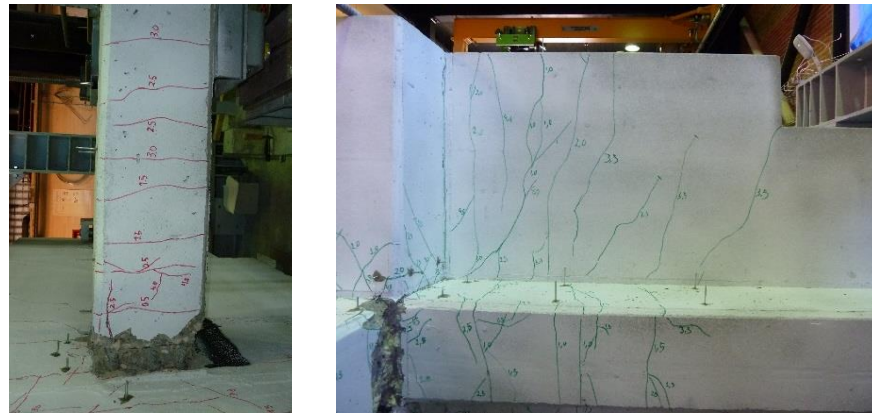


Fig. 6. Final damage state in C-EC8; left: superior column, right: beam underside

3.2 Retrofit specimen

The aim of the combined retrofit and selective weakening scheme (RT-B-sw) is to achieve a strength increase up to 80% of C-EC8, with a similar failure mechanism and ductility. As shown in Fig. 7, the envisaged hierarchy of strengths from the retrofit design is confirmed, with damage spread along the length of the beams and slab, similarly to C-EC8, and no damage in the columns for the retrofitted specimen. The continuous FRP strengthening of the columns allows a symmetrical rotation of superior and inferior columns, which hence prevents the brittle single-storey failure observed for C1. No debonding of the FRP is observed throughout the test, while partial rupture in the beam FRP strand is noticed towards the end of the test (at 5.0% drift). The maximum recorded strain in the vertical FRP strands is significantly lower than the debonding or rupture strain (0.19%).

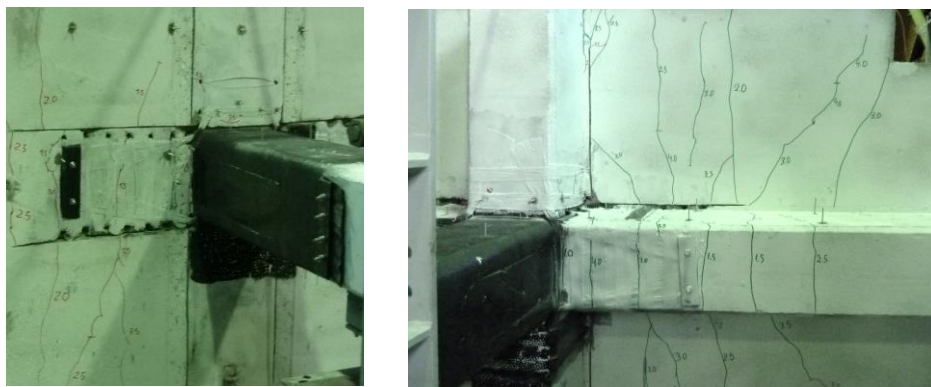


Fig. 7. Final damage state in C1-RT-B; left: column and slab, right: beam underside

In terms of the global force-drift envelope and energy dissipation (Fig. 8), the performance of C1-RT-B-sw presents a large improvement compared to C1, with a similar performance to the target 80% of C-EC8. Rather than the target 80%, 70.1% of the strength of C-EC8 is achieved by the retrofitted specimen. Still, this corresponds to a significant strength increase of 37.7% with respect to C1, despite a lower concrete strength than the two control specimens and severe reinforcement design deficiencies.

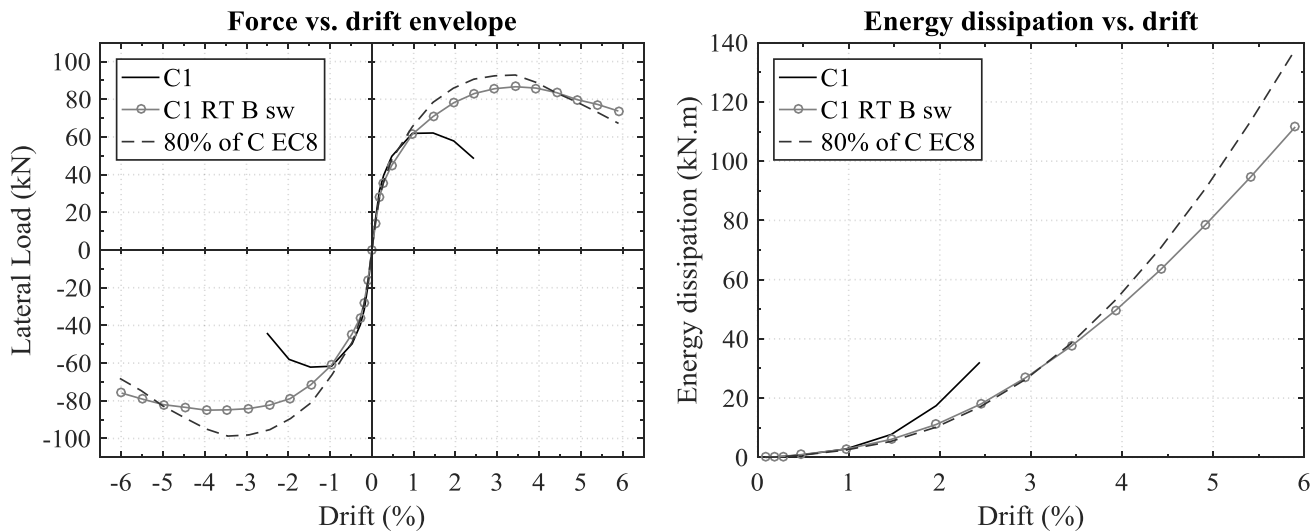


Fig. 8. Force-drift envelope and energy dissipation against drift for all specimens

A more ductile failure mechanism, with damage in the beams starting from the predicted plastic hinge zone (450 mm away from the beam-joint interface), is observed. The ductile failure is confirmed by the highest ductility recorded for C1-RT-B-sw (6.1, +89.6% compared to C1). The observed failure mechanism is a direct consequence of the selective weakening of the slab. A stronger participation of the beams is observed in the failure mechanism, with larger beam rotation, even compared to C-EC8. This observation is further validated by the energy dissipation plots at component level in Fig. 9. For C1, only 2.4% of the total cumulative energy is dissipated by the beams and slab, while for C-EC8 (12.4%) and C1-RT-B-sw (14.4%) a more significant proportion of the total energy dissipation is attributable to the beams.

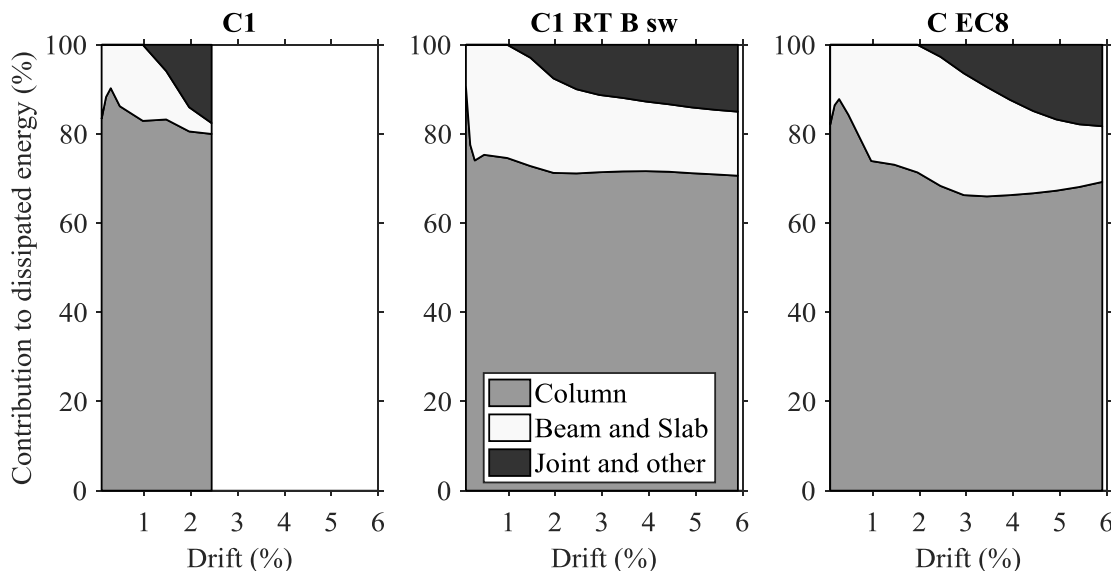


Fig. 9. Relative contribution to the total dissipated energy by component for each specimen

Finally, next to the largest ductility, the largest yield drift (0.95%, +46% compared to C1) is also observed for the retrofitted specimen as a consequence of the strengthening intervention. This, in turn, is favourable as it would reduce the need for repair in the case of less significant earthquakes. The lowest inter-cycle strength degradation (-61.8% compared to C1) and post-peak softening slopes (-61.8%) are also seen for C1-RT-B-sw, indicating a significantly improved performance under cyclic loading and improved residual strength, respectively.

4. Conclusions

In the aftermath of recent earthquakes (e.g. L'Aquila 2009), an abundant use of strengthening with FRP is observed. Despite the increasing popularity of using FRP sheets for the seismic retrofit of RC structures, only limited experimental studies on the retrofit of beam-column joints with realistic geometry exist in the literature. The omission of slabs and transverse beams from the experimental set-ups represents an unrealistic depiction of real structural retrofit issues and needs. The need for a more realistic experimental set-up is addressed in this paper, as three full-scale interior beam-column joint with slab and transverse beams are tested under cyclic loading to provide further empirical evidence for a realistic FRP retrofit solution.

The tested behaviour of a non-seismically designed control specimen is characterised by a brittle single-storey failure. For a specimen designed to modern guidelines, a more ductile and dissipative behaviour, with increased beam damage, is observed. The results from the specimen designed to modern guidelines is used as a benchmark for a realistic retrofit design and helps to identify strengthening objectives. While the change in failure mechanism and associated increased ductility are deemed achievable targets, the increase in strength observed for C-EC8 is not realistic for the retrofit of existing deficient structures.

A realistic FRP retrofit strategy for specimens with typical pre-1970's deficiencies is proposed with the aim of increasing the lateral load capacity and ductility of a structure. In contrast to many studies in the literature, the proposed retrofit takes into account a realistic structural geometry and the obstacles associated to it. Combined CFRP strengthening of columns, beams and joint with selective weakening is performed to enhance the flexural capacity of the columns and relocate the formation of a plastic hinge to the beam, and away from the joint interface.

In the literature, average increases in strength between 21.5% (for specimens with slab) and 46.1% (for specimens without slab) are observed. For retrofit RT-B-sw, an observed increase of 37.7% compared to C1 is hence a significant improvement even with respect to the performance of other FRP retrofits. This proves that the proposed novel retrofit lay-out can be very effective even when a realistic set-up is considered.

Overall, while the target strength of 80% of C-EC8 may not be fully achieved for C1-RT-B-sw, the very ductile failure mechanism has improved the seismic behaviour in terms of all measured diagnostics. The combined selective weakening and FRP retrofit can be seen as a successful intervention for structures with significant design deficiencies. The combination of fan-shaped splaying of the strands, mechanical anchorage with steel plates and FRP anchorage with horizontal wraps proves successful in avoiding significant debonding. Finally, the FRP retrofit scheme presented in this study successfully takes into account realistic specimen geometry, reflecting challenges in real structures. The practical implementation of the retrofit is demonstrated and can hence be seen as a readily applicable retrofit solution.

5. Acknowledgements

This research is funded as part of the Challenging RISK project funded by EPSRC (EP/K022377/1). The authors acknowledge the staff of the Civil Laboratory at the University of Aveiro for the support during the experimental campaign. The CFRP used in the experiments is kindly provided by S&P reinforcement.

6. References

- [1] Ricci P, De Luca F, Verderame GM (2011): 6th April 2009 L'Aquila earthquake, Italy: reinforced concrete building performance. *Bulletin of Earthquake Engineering*, **9**(1), 285–305.



- [2] Bousselham A (2010): State of Research on Seismic Retrofit of RC Beam-Column Joints with Externally Bonded FRP. *Journal of Composites for Construction*, **14**(1), 49–61.
- [3] Choudhury AM, Deb SK, Dutta A (2013): Study on size effect of fibre reinforced polymer retrofitted reinforced concrete beam–column connections under cyclic loading. *Canadian Journal of Civil Engineering*, **40**(4), 353–360.
- [4] Park S, Mosalam KM (2013): Experimental Investigation of Nonductile RC Corner Beam-Column Joints with Floor Slabs. *Journal of Structural Engineering*, **139**(1), 1–14.
- [5] Antonopoulos C, Triantafillou T (2003): Experimental Investigation of FRP-Strengthened RC Beam-Column Joints. *Journal of Composites for Construction*, **7**(1), 39–49.
- [6] Pohoryles D, Melo J, Rossetto T, Varum H (2015): Experimental investigation on the seismic FRP retrofit of full-scale RC beam-column joints. *Improving the Seismic Performance of Existing Buildings and Other Structures, 2nd ATC-SEI conference on improving the seismic performance of existing buildings and other structures*. San Francisco, California: ASCE.
- [7] Pohoryles DA, Rossetto T, Melo J, Varum H (2016): A combined FRP and selective weakening retrofit for realistic pre-1970's RC structures, *ICONHIC 2016 - 1st International Conference on Natural Hazards & Infrastructure*. Chania, Greece.
- [8] Akguzel U, Pampanin S (2010): Effects of Variation of Axial Load and Bidirectional Loading on Seismic Performance of GFRP Retrofitted Reinforced Concrete Exterior Beam-Column Joints. *Journal of Composites for Construction*, **14**(1), 94–104.
- [9] CEN (2004): BS EN 1998-1:2004 Eurocode 8. Design of structures for earthquake resistance. General rules, seismic actions and rules for buildings.
- [10] ACI (2008): *ACI 440.2R-08 - Guide for the design and construction of externally bonded FRP systems for strengthening concrete structures*. Farmington Hills, Mich.: American Concrete Institute.
- [11] CNR (2013): DT 200.R1/2013 - Guide for the Design and Construction of Externally Bonded FRP Systems for Strengthening Existing Structures - Materials, RC and PC structures, masonry structures.
- [12] Shiohara H, Kusuhara F, Tajiri S, Fukuyama H (2009): Seismic Retrofit of Reinforced Concrete Beam-Column Joints with CFRP Composites. *Improving the Seismic Performance of Existing Buildings and Other Structures, ATC & SEI 2009 Conference on Improving the Seismic Performance of Existing Buildings and Other Structures*. San Francisco, California: American Society of Civil Engineers.
- [13] Pampanin S, Akguzel U (2011): Performance-Based Seismic Retrofit of Existing Reinforced Concrete Frame Buildings using Fibre-Reinforced Polymers: Challenges and Solutions. *Structural Engineering International*, **21**(3), 260–270.
- [14] ACI (2014): *ACI 440-F - Seismic Strengthening of Concrete Buildings Using FRP Composites (draft)*.
- [15] Park YJ, Ang AH, Wen YK (1987): Damage-limiting aseismic design of buildings. *Earthquake Spectra*, **3**(1), 1–26.
- [16] Rossetto T, Pohoryles DA, Melo J, Varum H (2017): The effect of slab and transverse beams on the behaviour of full-scale pre-1970's RC beam-column joints. *Proceedings of the 16th World Conference on Earthquake Engineering, 16th World Conference on Earthquake Engineering*. Santiago, Chile.